

Anderson-Bogoliubov and Carlson-Goldman modes in counterflow superconductors. The case study of a double monolayer graphene.

K. V. Germash¹, D. V. Fil^{1,2*}

¹*Institute for Single Crystals, National Academy of Sciences of Ukraine, 60 Nauky Avenue, Kharkiv 61072, Ukraine*

²*V.N. Karazin Kharkiv National University, 4 Svobody Square, Kharkiv 61022, Ukraine*

The impact of electron-hole pairing on the spectrum of plasma excitations of double layer systems is investigated. The approach accounts coupling of the scalar potential oscillations with fluctuations of the order parameter Δ . The theory is developed with reference to a double monolayer graphene. We find that the spectrum of antisymmetric (acoustic) plasma excitations contains a weakly damped mode below the gap 2Δ and a strongly damped mode above the gap. The lower mode can be interpreted as an analog of the Carlson-Goldman mode. This mode has an acoustic dispersion relation at small wave vectors and it saturates at the level 2Δ at large wave vectors. Its velocity is larger than the velocity of the Anderson-Bogoliubov mode $v_{AB} = v_F/\sqrt{2}$, and it can be smaller as well as larger than the Fermi velocity v_F . The damping rate of this mode strongly increases under increase in temperature. Out-of-phase oscillations of the order parameters of two spin components are also analyzed. This part of the spectrum contains two modes one of which is recognized as the Anderson-Bogoliubov (phase) mode and the other, as the Schmid (amplitude) mode. With minor modifications the theory describes collective modes in the double bilayer graphene system as well.

I. INTRODUCTION

Electron-hole pairing is a phenomenon analogous to the Cooper pairing that may occur in double layer systems consisting of an electron-doped and a hole-doped conducting layers^{1,2} (see also Ref. 3 for a review). In the paired state the system may support dissipationless counterflow - a flow of oppositely directed superconducting electric currents in adjacent layers. The phenomenon is referred to as the superfluidity of spatially indirect excitons or the counterflow superconductivity.

The counterflow superconductivity was observed⁴⁻⁶ in quantum Hall bilayers with the total filling factor of Landau levels $\nu_1 + \nu_2 = 1$ (see Ref. 7 for recent development). In addition, quantum Hall bilayers demonstrate a zero bias peak in the differential tunnel conductance⁸ and a strong interlayer drag resistance⁹. These two features are also considered as experimental signatures of the electron-hole pairing. Similar features were observed in electron-hole bilayers in zero magnetic field. The increase of the interlayer drag resistance at low temperatures was detected in a double quantum well in AlGaAs heterostructures^{10,11} and in hybrid double-layer systems comprising a monolayer (bilayer) graphene in close proximity to a quantum well created in GaAs¹². Experimental observation of strongly enhanced tunneling between graphene bilayers was reported recently¹³. At low temperature and equal occupation of graphene bilayers by electrons and holes a tunneling conductance at small bias voltage was many orders of magnitude greater than that predicted for uncorrelated electrons and holes¹³.

Theoretical considerations show that promising candidates for a realization of electron-hole pairing in zero magnetic field are double monolayer¹⁴⁻¹⁹, double bilayer²⁰⁻²² and double multilayer²³ graphenes, double transition metal dichalcogenide monolayers²⁴⁻²⁶, phosphorene double layer²⁷ and topological insulators^{28,29}.

In our recent papers³⁰⁻³² we have found the effects that can be considered as additional hallmarks of the electron-hole pairing. It was shown³⁰ that the electron-hole pairing suppresses the ability of a double layer graphene system to screen the electrostatic field of an external charge. In the paired state at $T = 0$ the electrostatic field remains completely unscreened at large distances. It was found³¹ that the electron-hole pairing influences significantly the plasmon spectrum of the system. Instead of one optical mode two plasmon modes emerge. The frequency of the lower mode is very sensitive to the temperature and it disappears at $T = 0$. It was established³² that the electron-hole pairing provokes a huge increase of efficiency of the third-harmonic generation in double monolayer and double bilayer graphenes.

The results³⁰⁻³² were obtained within the approach that does not account the fluctuations of the order parameter of the electron-hole pairing. It is known from the Bardin-Cooper-Schrieffer (BCS) theory of superconductivity^{33,34} that neglecting the order parameter oscillations results in a violation of gauge invariancy of the polarization matrix. The gauge invariance is restored by “dressing” of the vertexes. The “dressed” vertexes should satisfy the generalized Ward identity. In Ref. 31 we have proposed a heuristic approach to the problem. We have obtained the gauge invariant polarization matrix using the vertex functions obtained as particular solutions of the generalized Ward identity.

In this paper we present the approach in which the order parameter fluctuations are accounted explicitly. Our approach is close to one developed in Ref. 35 for conventional superconductors.

II. THE MODEL

We describe the electron-hole pairing in a double monolayer graphene system in the framework of the constant gap model^{16,17}. In this model the order parameter of the electron-hole pairing is independent of the momentum. The model can be formulated self-consistently under assumption that the interaction between electrons and holes is local in space. In the constant gap model the relation between the order parameter and scalar potential oscillations is given by algebraic equations. The Hamiltonian of the model has the form

$$H = H_1 + H_2 + H_C, \quad (1)$$

where

$$H_n = -t \sum_{\sigma} \sum_{\langle ij \rangle} c_{n,i,\sigma}^+ c_{n,j,\sigma} - \mu_n \sum_{i,\sigma} c_{n,i,\sigma}^+ c_{n,i,\sigma} \quad (2)$$

is the single-layer Hamiltonian, $c_{n,i,\sigma}^+$ and $c_{n,i,\sigma}$ are the creation and annihilation operators of electrons, $n = 1, 2$ is the layer index, i is the lattice site index, $\sigma = \pm 1/2$ is the spin index, t is the nearest-neighbor hopping energy, and μ_n is the electron chemical potential in the n -th layer. The chemical potentials counted from the Dirac points satisfy the condition $\mu_1 = -\mu_2 = \mu$ that corresponds to equal concentration of electrons and holes. The interaction part of

the Hamiltonian reads

$$H_C = V \sum_{i,\sigma} c_{1,i,\sigma}^+ c_{2,i,\sigma}^+ c_{2,i,\sigma} c_{1,i,\sigma}, \quad (3)$$

where V is the interaction constant ($V > 0$).

The order parameter of the electron-hole pairing is defined as

$$\Delta_{i,\sigma} = V \langle c_{2,i,\sigma}^+ c_{1,i,\sigma} \rangle. \quad (4)$$

The order parameter can be presented as a sum of the equilibrium part $\Delta_{i,\sigma}^{(0)}$ and the fluctuating part $\Delta_{i,\sigma}^{(fl)}(t)$. We set $\Delta_{i_A,\sigma}^{(0)} = -\Delta_{i_B,\sigma}^{(0)} = \Delta_0$, where i_A and i_B stand for the sites in the i -th unit cell belonging to two different graphene sublattices. Such a choice corresponds to the paired state with the lowest energy^{16,17}.

Neglecting the order parameter fluctuations we obtain the mean-field Hamiltonian

$$H_{MF} = H_1 + H_2 - \sum_{i,\sigma} (\Delta_0 c_{1,i_A,\sigma}^+ c_{2,i_A,\sigma} - \Delta_0 c_{1,i_B,\sigma}^+ c_{2,i_B,\sigma} + H.c.), \quad (5)$$

Applying the Fourier-transformation to the Hamiltonian (5) and considering one spin component we get

$$H_{MF} = \sum_{\mathbf{k}} \Psi_{\mathbf{k}}^+ h_{\mathbf{k}} \Psi_{\mathbf{k}} = \sum_{\mathbf{k}} (c_{1,A,\mathbf{k}}^+ c_{1,B,\mathbf{k}}^+ c_{2,A,\mathbf{k}}^+ c_{2,B,\mathbf{k}}^+) \begin{pmatrix} -\mu & f_{\mathbf{k}} & -\Delta_0 & 0 \\ f_{\mathbf{k}}^* & -\mu & 0 & \Delta_0 \\ -\Delta_0 & 0 & \mu & f_{\mathbf{k}} \\ 0 & \Delta_0 & f_{\mathbf{k}}^* & \mu \end{pmatrix} \begin{pmatrix} c_{1,A,\mathbf{k}} \\ c_{1,B,\mathbf{k}} \\ c_{2,A,\mathbf{k}} \\ c_{2,B,\mathbf{k}} \end{pmatrix}, \quad (6)$$

where $c_{n,A(B),\mathbf{k}} = (1/\sqrt{N}) \sum_i c_{n,i_A(B)} e^{i\mathbf{k}\mathbf{R}_i}$ (here spin index is omitted), N is the number of unit cells, $f_{\mathbf{k}} = |f_{\mathbf{k}}| e^{i\chi_{\mathbf{k}}} = -t \sum_{j=1,2,3} e^{-i\mathbf{k}\vec{\delta}_j}$, and $\vec{\delta}_1 = \mathbf{a}_1$, $\vec{\delta}_2 = \mathbf{a}_2$, $\vec{\delta}_3 = 0$ (\mathbf{a}_1 and \mathbf{a}_2 are the lattice vectors).

The Hamiltonian (6) is diagonalized by the unitary transformation

$$H_{MF} = \sum_{\mathbf{k}} \Psi_{\mathbf{k}}^+ \hat{U}_{\mathbf{k}}^{-1} \hat{U}_{\mathbf{k}} h_{\mathbf{k}} \hat{U}_{\mathbf{k}}^{-1} \hat{U}_{\mathbf{k}} \Psi_{\mathbf{k}} = \sum_{\mathbf{k}} \tilde{\Psi}_{\mathbf{k}}^+ \tilde{h}_{\mathbf{k}} \tilde{\Psi}_{\mathbf{k}}, \quad (7)$$

where $\tilde{h}_{\mathbf{k}} = \hat{U}_{\mathbf{k}} h_{\mathbf{k}} \hat{U}_{\mathbf{k}}^{-1}$. The matrix $\hat{U}_{\mathbf{k}}$ can be written in a form of the product

$$\hat{U}_{\mathbf{k}} = \hat{U}_{uv} \hat{U}_b \hat{U}_{\chi}. \quad (8)$$

The matrix

$$\hat{U}_{\chi} = \frac{1}{\sqrt{2}} \begin{pmatrix} 1 & e^{i\chi_{\mathbf{k}}} & 0 & 0 \\ 1 & -e^{i\chi_{\mathbf{k}}} & 0 & 0 \\ 0 & 0 & 1 & e^{i\chi_{\mathbf{k}}} \\ 0 & 0 & 1 & -e^{i\chi_{\mathbf{k}}} \end{pmatrix} \quad (9)$$

diagonalizes the single-layer parts of the Hamiltonian. The matrix

$$\hat{U}_b = \begin{pmatrix} 1 & 0 & 0 & 0 \\ 0 & 0 & 0 & 1 \\ 0 & 1 & 0 & 0 \\ 0 & 0 & 1 & 0 \end{pmatrix} \quad (10)$$

rearranges the elements of the matrix $\hat{U}_{\chi} h_{\mathbf{k}} \hat{U}_{\chi}^{-1}$ into two blocks:

$$\hat{U}_b \hat{U}_{\chi} h_{\mathbf{k}} \hat{U}_{\chi}^{-1} \hat{U}_b^{-1} = \begin{pmatrix} \xi_{\mathbf{k},+1} & -\Delta_0 & 0 & 0 \\ -\Delta_0 & -\xi_{\mathbf{k},+1} & 0 & 0 \\ 0 & 0 & \xi_{\mathbf{k},-1} & -\Delta_0 \\ 0 & 0 & -\Delta_0 & -\xi_{\mathbf{k},-1} \end{pmatrix}, \quad (11)$$

where $\xi_{\mathbf{k},\lambda} = \lambda |f_{\mathbf{k}}| - \mu$, and $\lambda = \pm 1$.

Each block can be diagonalized by the u-v transformation. The matrix

$$\hat{U}_{uv} = \begin{pmatrix} u_{\mathbf{k},+1} & -v_{\mathbf{k},+1} & 0 & 0 \\ v_{\mathbf{k},+1} & u_{\mathbf{k},+1} & 0 & 0 \\ 0 & 0 & u_{\mathbf{k},-1} & -v_{\mathbf{k},-1} \\ 0 & 0 & v_{\mathbf{k},-1} & u_{\mathbf{k},-1} \end{pmatrix} \quad (12)$$

is expressed through the coefficients of this transformation:

$$u_{\mathbf{k},\lambda} = \sqrt{\frac{1}{2} \left(1 + \frac{\xi_{\mathbf{k},\lambda}}{E_{\mathbf{k},\lambda}} \right)}, \quad v_{\mathbf{k},\lambda} = \sqrt{\frac{1}{2} \left(1 - \frac{\xi_{\mathbf{k},\lambda}}{E_{\mathbf{k},\lambda}} \right)}, \quad (13)$$

where $E_{\mathbf{k},\lambda} = \sqrt{\xi_{\mathbf{k},\lambda}^2 + \Delta_0^2}$.

The transformed Hamiltonian has the diagonal form

$$\tilde{h}_{\mathbf{k}} = \begin{pmatrix} E_{\mathbf{k},+1} & 0 & 0 & 0 \\ 0 & -E_{\mathbf{k},+1} & 0 & 0 \\ 0 & 0 & E_{\mathbf{k},-1} & 0 \\ 0 & 0 & 0 & -E_{\mathbf{k},-1} \end{pmatrix}. \quad (14)$$

The spectrum of quasiparticle excitations $\pm E_{\mathbf{k},\lambda}$ contains two bands with positive energies and two bands with negative energies. To present the results in a compact form we introduce the notations $E_{\nu} = E_{\mathbf{k},\lambda,m} = mE_{\mathbf{k},\lambda}$ ($m = \pm 1$) and $\nu = (\mathbf{k}, \lambda, m)$. The latter quantity is the full set of the quasiparticle quantum numbers, excluding spin.

The order parameter can be expressed through the quasiparticle creation and annihilation operators α_{ν}^+ , α_{ν} :

$$\Delta_0 = \frac{U}{4N} \sum_{\nu} \Delta_{\nu\nu} \langle \alpha_{\nu}^+ \alpha_{\nu} \rangle, \quad (15)$$

where $\Delta_{\nu\nu}$ are the diagonal elements of the matrix

$$\Delta_{\nu\nu'} = \hat{U}_{\mathbf{k}} \begin{pmatrix} 0 & \hat{\sigma}_z \\ \hat{\sigma}_z & 0 \end{pmatrix} \hat{U}_{\mathbf{k}'}^{-1} \quad (16)$$

and $\hat{\sigma}_z$ is the Pauli matrix.

Calculating the matrix (16) and replacing the averages $\langle \alpha_{\nu}^+ \alpha_{\nu} \rangle$ with the Fermi distribution function we arrive at the self-consistency equation for the order parameter

$$\Delta_0 = \frac{V\Omega_0}{2S} \sum_{\mathbf{k},\lambda} \frac{\Delta_0}{2E_{\mathbf{k},\lambda}} \tanh \frac{E_{\mathbf{k},\lambda}}{2T}, \quad (17)$$

where Ω_0 is the area of the unit cell and S is the area of the system.

We emphasize that Eq. (17) differs from one obtained in the model with a long-range Coulomb interaction^{14,15,18,19}. In the latter case the self-consistency equation has the form

$$\Delta_{\mathbf{k},\lambda} = \frac{1}{S} \sum_{\mathbf{k}',\lambda'} V(\mathbf{k} - \mathbf{k}') \frac{1 + \lambda \lambda' \cos(\chi_{\mathbf{k}} - \chi_{\mathbf{k}'})}{2} \frac{\Delta_{\mathbf{k}',\lambda'}}{2E_{\mathbf{k}',\lambda'}} \tanh \frac{E_{\mathbf{k}',\lambda'}}{2T}, \quad (18)$$

where $V(\mathbf{q})$ is the Fourier-component of the interlayer Coulomb interaction. In difference with Eq. (17), the order parameter independent of \mathbf{k} and λ ($\Delta_{\mathbf{k},\lambda} = \Delta_0$) does not satisfy Eq. (18).

III. PERTURBATION HAMILTONIAN

Now we add to the Hamiltonian (6) the perturbation part H_{int} . The perturbation Hamiltonian H_{int} describes the fluctuations of the order parameter and the interaction of electrons with the scalar potential $\varphi(\mathbf{r}, t)$. We consider the fluctuations for which $\Delta_{i_A,\sigma}^{(fl)}(t) = -\Delta_{i_B,\sigma}^{(fl)}(t) = \Delta_{i,\sigma}^{(fl)}(t)$ (here i is the unit cell index) and do not account fluctuations with $\Delta_{i_A,\sigma}^{(fl)} = \Delta_{i_B,\sigma}^{(fl)}$. The latter ones are decoupled from the scalar potential oscillations and do not modify the response to the electromagnetic field.

The Fourier-components of the real and imaginary parts of the order parameter fluctuations are defined as

$$\Delta_1(\mathbf{q}, \omega) = \Omega_0 \sum_i \int dt e^{i\omega t - i\mathbf{q}\mathbf{R}_i} \text{Re}[\Delta_i^{(fl)}(t)], \quad (19)$$

$$\Delta_2(\mathbf{q}, \omega) = \Omega_0 \sum_i \int dt e^{i\omega t - i\mathbf{q}\mathbf{R}_i} \text{Im}[\Delta_i^{(fl)}(t)]. \quad (20)$$

Taking in mind that Δ_0 is a real-valued quantity one finds that fluctuations Δ_1 and Δ_2 (if they are small) describe the amplitude and the phase oscillations of the order parameter, respectively.

The perturbation Hamiltonian can be presented in the matrix form

$$H_{int}(t) = -\frac{1}{2\pi S} \sum_{\mathbf{k}, \mathbf{q}} \int d\omega e^{-i\omega t} \Psi_{\mathbf{k}-\mathbf{q}}^+ \left[\frac{e}{2} \varphi_+(\mathbf{q}, \omega) \hat{T}^{(0)} + \Delta_1(\mathbf{q}, \omega) \hat{T}^{(1)} + \Delta_2(\mathbf{q}, \omega) \hat{T}^{(2)} + \frac{e}{2} \varphi_-(\mathbf{q}, \omega) \hat{T}^{(3)} \right] \Psi_{\mathbf{k}}, \quad (21)$$

where the operators $\Psi_{\mathbf{k}}^+$ and $\Psi_{\mathbf{k}}$ are defined in Eq. (6),

$$\varphi_{\pm}(\mathbf{q}, \omega) = \Omega_0 \sum_i \int dt e^{i\omega t - i\mathbf{q}\mathbf{R}_i} [\varphi_1(\mathbf{R}_i, t) \pm \varphi_2(\mathbf{R}_i, t)] \quad (22)$$

are the Fourier-components of the scalar potential, and $\varphi_{1(2)}(\mathbf{R}_i, t)$ is the scalar potentials in the graphene layer 1(2) in the i -th unit cell. The matrixes $\hat{T}^{(s)}$ in Eq. (21) are expressed through the Pauli matrix $\hat{\sigma}_z$ and the identity matrix \hat{I} :

$$\hat{T}^{(0)} = \begin{pmatrix} \hat{I} & 0 \\ 0 & \hat{I} \end{pmatrix}, \quad \hat{T}^{(1)} = \begin{pmatrix} 0 & \hat{\sigma}_z \\ \hat{\sigma}_z & 0 \end{pmatrix}, \quad \hat{T}^{(2)} = \begin{pmatrix} 0 & i\hat{\sigma}_z \\ -i\hat{\sigma}_z & 0 \end{pmatrix}, \quad \hat{T}^{(3)} = \begin{pmatrix} \hat{I} & 0 \\ 0 & -\hat{I} \end{pmatrix}. \quad (23)$$

We apply the transformation (7) to the Hamiltonian (21) and write it through the operators of creation and annihilation of quasiparticle excitations:

$$H_{int}(t) = \frac{1}{2\pi S} \sum_{\nu_1, \nu_2} \int d\omega e^{-i\omega t} \alpha_{\nu_1}^+ [h_{int}(\omega)]_{\nu_1, \nu_2} \alpha_{\nu_2}, \quad (24)$$

where

$$[h_{int}(\omega)]_{\nu_1, \nu_2} = -\frac{e}{2} \varphi_+(\mathbf{k}_2 - \mathbf{k}_1, \omega) R_{\nu_1, \nu_2}^{(0)} - \Delta_1(\mathbf{k}_2 - \mathbf{k}_1, \omega) R_{\nu_1, \nu_2}^{(1)} - \Delta_2(\mathbf{k}_2 - \mathbf{k}_1, \omega) R_{\nu_1, \nu_2}^{(2)} - \frac{e}{2} \varphi_-(\mathbf{k}_2 - \mathbf{k}_1, \omega) R_{\nu_1, \nu_2}^{(3)}, \quad (25)$$

the matrixes $R_{\nu_1, \nu_2}^{(s)}$ ($s = 0, 1, 2, 3$) are given by the equation

$$R_{\mathbf{k}_1, \lambda_1, m_1; \mathbf{k}_2, \lambda_2, m_2}^{(s)} = \frac{1 + \lambda_1 \lambda_2 e^{i(\chi_{\mathbf{k}_1} - \chi_{\mathbf{k}_2})}}{2} [M^{(s)}(\mathbf{k}_1, \lambda_1, \mathbf{k}_2, \lambda_2)]_{i_{m_1}, i_{m_2}}, \quad (26)$$

and the matrixes $\hat{M}^{(s)}$ are expressed through the product

$$\hat{M}^{(s)}(\mathbf{k}_1, \lambda_1, \mathbf{k}_2, \lambda_2) = \begin{pmatrix} u_{\mathbf{k}_1, \lambda_1} & -v_{\mathbf{k}_1, \lambda_1} \\ v_{\mathbf{k}_1, \lambda_1} & u_{\mathbf{k}_1, \lambda_1} \end{pmatrix} \sigma^{(s)} \begin{pmatrix} u_{\mathbf{k}_2, \lambda_2} & v_{\mathbf{k}_2, \lambda_2} \\ -v_{\mathbf{k}_2, \lambda_2} & u_{\mathbf{k}_2, \lambda_2} \end{pmatrix}. \quad (27)$$

Here $\hat{\sigma}^{(0)} = \hat{I}$, $\hat{\sigma}^{(1)} = \hat{\sigma}_x$, $\hat{\sigma}^{(2)} = -\hat{\sigma}_y$, $\hat{\sigma}^{(3)} = \hat{\sigma}_z$, and $i_{+1} = 1$, $i_{-1} = 2$.

IV. RESPONSE FUNCTIONS

Our system is described by the Hamiltonian

$$H(t) = H_0 + H_{int}(t) = \sum_{\nu, \sigma} E_{\nu} \alpha_{\nu, \sigma}^+ \alpha_{\nu, \sigma} + \frac{1}{2\pi S} \sum_{\nu_1, \nu_2, \sigma} \int d\omega e^{-i\omega t} \alpha_{\nu_1, \sigma}^+ [h_{int, \sigma}(\omega)]_{\nu_1, \nu_2} \alpha_{\nu_2, \sigma}, \quad (28)$$

where $[h_{int, \sigma}(\omega)]_{\nu_1, \nu_2}$ is given by Eq. (25) with $\Delta_{1(2)}(\mathbf{k}, \omega) \equiv \Delta_{1(2), \sigma}(\mathbf{k}, \omega)$.

To calculate the response of the system to the scalar potential and to the order parameter fluctuations we define the response functions

$$\eta_{\sigma}^{(s)}(\mathbf{q}, \omega) = \int dt e^{i\omega t} \sum_{\mathbf{k}} \langle \Psi_{\mathbf{k}+\mathbf{q}, \sigma}^+ \hat{T}^{(s)} \Psi_{\mathbf{k}, \sigma} \rangle, \quad (29)$$

where $\Psi_{\mathbf{k}, \sigma}^+$ and $\Psi_{\mathbf{k}, \sigma}$ are the same operators as in Eq. (6) with restored spin indexes. The angle brackets mean the quantum mechanical and thermodynamic average. We compute the averages in Eq. (29) using the density matrix formalism. The density matrix $\hat{\rho}(t)$ satisfies the equation

$$\frac{\partial \hat{\rho}(t)}{\partial t} = \frac{1}{i\hbar} [H(t), \hat{\rho}(t)] - \gamma(\hat{\rho}(t) - \hat{\rho}_0), \quad (30)$$

where $\hat{\rho}_0$ is the density matrix of the system described by the Hamiltonian H_0 , and γ is the relaxation rate. The averages in Eq. (29) are calculated as

$$\langle \Psi_{\mathbf{k}+\mathbf{q}, \sigma}^+ \hat{T}^{(s)} \Psi_{\mathbf{k}, \sigma} \rangle = \text{Tr} \left([\hat{\rho}(t)]_{\mathbf{k}, \sigma; \mathbf{k}+\mathbf{q}, \sigma} \hat{T}^{(s)} \right), \quad (31)$$

where the trace is taken over the sublattice and layer indexes.

In the quasiparticle basis the response functions (29) are expressed as

$$\eta_{\sigma}^{(s)}(\mathbf{q}, \omega) = \sum_{\nu_1, \nu_2} [\hat{\rho}(\omega)]_{\nu_1, \sigma; \nu_2, \sigma} R_{\nu_2, \nu_1}^{(s)} \delta_{\mathbf{k}_2, \mathbf{k}_1 + \mathbf{q}}, \quad (32)$$

where $\hat{\rho}(\omega) = \int dt \exp(i\omega t) \hat{\rho}(t)$ and the matrixes $R_{\nu_1, \nu_2}^{(s)}$ are given by Eq. (26).

The density matrix is sought in a form of expansion in powers of the perturbation Hamiltonian: $\hat{\rho}(\omega) = \hat{\rho}_0(\omega) + \hat{\rho}_1(\omega) + \dots$. The zero order term in this expansion is the equilibrium density matrix

$$[\hat{\rho}_0(\omega)]_{\nu_1, \sigma_1; \nu_2, \sigma_2} = 2\pi\delta(\omega)\delta_{\nu_1, \nu_2}\delta_{\sigma_1, \sigma_2}f_{\nu_1}, \quad (33)$$

where $f_{\nu} = (e^{E_{\nu}/T} + 1)^{-1}$ is the Fermi distribution function. The first order term reads

$$[\hat{\rho}_1(\omega)]_{\nu_1, \sigma; \nu_2, \sigma'} = \frac{1}{S} \frac{f_{\nu_1} - f_{\nu_2}}{E_{\nu_1} - E_{\nu_2} - \hbar(\omega + i\gamma)} [h_{int, \sigma}(\omega)]_{\nu_1, \nu_2} \delta_{\sigma, \sigma'}. \quad (34)$$

The response functions $\eta^{(0)}$ and $\eta^{(3)}$ at $\mathbf{q} \neq 0$ determine the charge density fluctuations $\rho_{\pm, \sigma} = \rho_{1, \sigma} \pm \rho_{2, \sigma}$:

$$\rho_{+, \sigma}(\mathbf{q}, \omega) = -e\eta_{\sigma}^{(0)}(\mathbf{q}, \omega), \quad \rho_{-, \sigma}(\mathbf{q}, \omega) = -e\eta_{\sigma}^{(3)}(\mathbf{q}, \omega). \quad (35)$$

Taking into account the definition of the order parameter Eq. (4) we obtain the relation between the order parameter fluctuations and the response functions $\eta^{(1(2))}$ at $\mathbf{q} \neq 0$:

$$\Delta_{1, \sigma}(\mathbf{q}, \omega) = g\eta_{\sigma}^{(1)}(\mathbf{q}, \omega), \quad \Delta_{2, \sigma}(\mathbf{q}, \omega) = g\eta_{\sigma}^{(2)}(\mathbf{q}, \omega), \quad (36)$$

where $g = V\Omega_0/4$ is the coupling constant.

Restricting with the linear response approximation we obtain from Eqs. (32), (34), (35), (36) the following matrix equation

$$\begin{pmatrix} e^{-1}\rho_{+, \sigma}(\mathbf{q}, \omega) \\ -g^{-1}\Delta_{1, \sigma}(\mathbf{q}, \omega) \\ -g^{-1}\Delta_{2, \sigma}(\mathbf{q}, \omega) \\ e^{-1}\rho_{-, \sigma}(\mathbf{q}, \omega) \end{pmatrix} = \begin{pmatrix} \Pi_{00}(\mathbf{q}, \omega) & \Pi_{01}(\mathbf{q}, \omega) & \Pi_{02}(\mathbf{q}, \omega) & \Pi_{03}(\mathbf{q}, \omega) \\ \Pi_{10}(\mathbf{q}, \omega) & \Pi_{11}(\mathbf{q}, \omega) & \Pi_{12}(\mathbf{q}, \omega) & \Pi_{13}(\mathbf{q}, \omega) \\ \Pi_{20}(\mathbf{q}, \omega) & \Pi_{21}(\mathbf{q}, \omega) & \Pi_{22}(\mathbf{q}, \omega) & \Pi_{23}(\mathbf{q}, \omega) \\ \Pi_{30}(\mathbf{q}, \omega) & \Pi_{31}(\mathbf{q}, \omega) & \Pi_{32}(\mathbf{q}, \omega) & \Pi_{33}(\mathbf{q}, \omega) \end{pmatrix} \begin{pmatrix} e\varphi_{+}(\mathbf{q}, \omega)/2 \\ \Delta_{1, \sigma}(\mathbf{q}, \omega) \\ \Delta_{2, \sigma}(\mathbf{q}, \omega) \\ e\varphi_{-}(\mathbf{q}, \omega)/2 \end{pmatrix}, \quad (37)$$

where the components of the polarization matrix are given by the expression

$$\Pi_{s_1 s_2}(\mathbf{q}, \omega) = \frac{1}{S} \sum_{\nu_1, \nu_2} \delta_{\mathbf{k}_2, \mathbf{k}_1 + \mathbf{q}} \Phi_{\nu_1 \nu_2}^{s_1 s_2} \frac{1 + \lambda_1 \lambda_2 \cos(\chi_{\mathbf{k}_1} - \chi_{\mathbf{k}_2})}{2} \frac{f_{\nu_1} - f_{\nu_2}}{E_{\nu_1} - E_{\nu_2} - \hbar(\omega + i\gamma)}. \quad (38)$$

The factors $\Phi_{\nu_1 \nu_2}^{s_1 s_2}$ in Eq. (38) are expressed through the matrix (27):

$$\Phi_{\nu_1 \nu_2}^{s_1 s_2} = [\hat{M}^{(s_1)}(\mathbf{k}_1, \lambda_1, \mathbf{k}_2, \lambda_2)]_{i_{m_1}, i_{m_2}} [\hat{M}^{(s_2)}(\mathbf{k}_2, \lambda_2, \mathbf{k}_1, \lambda_1)]_{i_{m_2}, i_{m_1}}, \quad (39)$$

(there is no summation over repeated indexes in Eq. (39)).

From Eq. (39) we obtain the following explicit expressions for $\Phi_{\nu_1 \nu_2}^{s_1 s_2}$:

$$\begin{aligned} \Phi_{\nu_1 \nu_2}^{00} &= \frac{1}{2} \left(1 + \frac{\xi_1 \xi_2 + \Delta_0^2}{E_1 E_2} \right), \quad \Phi_{\nu_1 \nu_2}^{01} = \frac{\Delta_0}{2} \left(\frac{1}{E_1} + \frac{1}{E_2} \right), \quad \Phi_{\nu_1 \nu_2}^{02} = i \frac{\Delta_0}{2} \frac{\xi_2 - \xi_1}{E_2 E_1}, \quad \Phi_{\nu_1 \nu_2}^{03} = \frac{1}{2} \left(\frac{\xi_2}{E_2} + \frac{\xi_1}{E_1} \right), \\ \Phi_{\nu_1 \nu_2}^{11} &= \frac{1}{2} \left(1 - \frac{\xi_1 \xi_2 - \Delta_0^2}{E_1 E_2} \right), \quad \Phi_{\nu_1 \nu_2}^{12} = \frac{i}{2} \left(\frac{\xi_1}{E_1} - \frac{\xi_2}{E_2} \right), \quad \Phi_{\nu_1 \nu_2}^{13} = -\frac{\Delta_0}{2} \frac{\xi_1 + \xi_2}{E_1 E_2}, \\ \Phi_{\nu_1 \nu_2}^{22} &= \frac{1}{2} \left(1 - \frac{\xi_1 \xi_2 + \Delta_0^2}{E_1 E_2} \right), \quad \Phi_{\nu_1 \nu_2}^{23} = i \frac{\Delta_0}{2} \left(\frac{1}{E_2} - \frac{1}{E_1} \right), \\ \Phi_{\nu_1 \nu_2}^{33} &= \frac{1}{2} \left(1 + \frac{\xi_1 \xi_2 - \Delta_0^2}{E_1 E_2} \right) \end{aligned} \quad (40)$$

and $\Phi_{\nu_1 \nu_2}^{s_2, s_1} = (\Phi_{\nu_1 \nu_2}^{s_1, s_2})^*$. Here we use the notations $\xi_i \equiv \xi_{\nu_i}$ and $E_i \equiv E_{\nu_i}$.

Taking into account symmetry properties of the expression under summation in Eq. (38) one can show that some elements of the polarization matrix, namely $\Pi_{01}(\mathbf{q}, \omega)$, $\Pi_{02}(\mathbf{q}, \omega)$, $\Pi_{03}(\mathbf{q}, \omega)$, $\Pi_{10}(\mathbf{q}, \omega)$, $\Pi_{20}(\mathbf{q}, \omega)$, and $\Pi_{30}(\mathbf{q}, \omega)$ are equal to zero exactly.

V. COLLECTIVE MODES

In the nonretarded approximation the scalar potential satisfies the Poisson equation

$$\nabla[\varepsilon(\mathbf{r}) \nabla \varphi(\mathbf{r}, t)] = -4\pi\rho(\mathbf{r}, t), \quad (41)$$

where $\varepsilon(\mathbf{r})$ is the space-dependent dielectric constant. We imply that the system consists of two graphene layers separated by a dielectric layer with the dielectric constant ε and surrounded by a medium with $\varepsilon = 1$. Then

$$\varepsilon(\mathbf{r}) = \begin{cases} 1, & z < -d/2; \\ \varepsilon, & -d/2 < z < d/2; \\ 1, & z > d/2, \end{cases} \quad (42)$$

where d is the distance between graphene layers, and the z -axis is directed perpendicular to graphene layers.

To obtain the eigenmode spectrum we substitute into Eq. (41) the charge density in the form

$$\rho(\mathbf{r}, t) = \sum_{\sigma} [\rho_{1,\sigma}(\mathbf{r}_{pl}, t) \delta(z - d/2) + \rho_{2,\sigma}(\mathbf{r}_{pl}, t) \delta(z + d/2)], \quad (43)$$

where \mathbf{r}_{pl} is two-dimensional radius-vector in the (x, y) -plane. The charges $\rho_{n,\sigma}$ in Eq. (43) are the charges induced by the scalar potential and order parameter oscillations.

Making the Fourier-transformation of Eq. (41) we obtain the equation for $\varphi(\mathbf{q}, z, \omega)$. Its solution yields the relation between the potentials $\varphi_{\pm}(\mathbf{q}, \omega) = \varphi(\mathbf{q}, d/2, \omega) \pm \varphi(\mathbf{q}, -d/2, \omega)$ and the charge densities $\rho_{\pm}(\mathbf{q}, \omega) = \sum_{\sigma} \rho_{\pm,\sigma}(\mathbf{q}, \omega)$:

$$e^2 \varphi_{\pm}(\mathbf{q}, \omega) = V_{\pm}(q) \rho_{\pm}(\mathbf{q}, \omega), \quad (44)$$

where

$$V_{\pm}(q) = \frac{4\pi e^2}{q} \frac{1 \pm e^{-qd}}{(\varepsilon + 1) \mp (\varepsilon - 1)e^{-qd}} \quad (45)$$

are the Fourier components of the Coulomb interaction energies $V_{\pm}(r_{pl}) = V_{11}(r_{pl}) \pm V_{12}(r_{pl})$. Here $V_{11}(r_{pl})$ and $V_{12}(r_{pl})$ are the energies of interaction of two electrons located in the same and different layers, correspondingly (we account that in the uniform dielectric environment $V_{11}(r_{pl}) = V_{22}(r_{pl})$).

From Eqs. (37) and (44) we get the equation for the scalar potential and order parameter fluctuations:

$$\begin{pmatrix} 2\Pi_{00} - \frac{2}{V_+(q)} & 0 & 0 & 0 & 0 & 0 \\ 0 & \Pi_{11} + \frac{1}{g} & \Pi_{12} & 0 & 0 & \Pi_{13} \\ 0 & \Pi_{21} & \Pi_{22} + \frac{1}{g} & 0 & 0 & \Pi_{23} \\ 0 & 0 & 0 & \Pi_{11} + \frac{1}{g} & \Pi_{12} & \Pi_{13} \\ 0 & 0 & 0 & \Pi_{21} & \Pi_{22} + \frac{1}{g} & \Pi_{23} \\ 0 & \Pi_{31} & \Pi_{32} & \Pi_{31} & \Pi_{32} & 2\Pi_{33} - \frac{2}{V_-(q)} \end{pmatrix} \begin{pmatrix} e\varphi_+(\mathbf{q}, \omega)/2 \\ \Delta_{1,\uparrow}(\mathbf{q}, \omega) \\ \Delta_{2,\uparrow}(\mathbf{q}, \omega) \\ \Delta_{1,\downarrow}(\mathbf{q}, \omega) \\ \Delta_{2,\downarrow}(\mathbf{q}, \omega) \\ e\varphi_-(\mathbf{q}, \omega)/2 \end{pmatrix} = 0, \quad (46)$$

where $\Pi_{\alpha\beta} \equiv \Pi_{\alpha\beta}(\mathbf{q}, \omega)$, $\uparrow \equiv +\frac{1}{2}$, and $\downarrow \equiv -\frac{1}{2}$.

We calculate the polarization functions Eq. (38) applying the Dirac approximation for the electron spectrum. In this approximation the sum over \mathbf{k} is replaced with the integral over two separate circles in the Brillouin zone centered at the Dirac points K and K' . In these circles $|f(\mathbf{k})| \approx \hbar v_F k'$, and $\chi_{\mathbf{k}} \approx \mp \theta_{\mathbf{k}'}$, where \mathbf{k}' is counted from the corresponding Dirac point, $\theta_{\mathbf{k}'}$ is the angle between \mathbf{k}' and the x -axis, and v_F is the Fermi velocity in graphene. The shortage of the Dirac approximation is that the integrals in the expressions for $\Pi_{11}(\mathbf{q}, \omega)$ and $\Pi_{22}(\mathbf{q}, \omega)$ diverge at $k' \rightarrow \infty$. To overcome this difficulty we account the equality

$$\frac{1}{g} = \frac{1}{S} \sum_{\mathbf{k}, \lambda} \frac{1}{E_{\mathbf{k}, \lambda}} \tanh \frac{E_{\mathbf{k}, \lambda}}{2T} = -\frac{1}{S} \sum_{m, \mathbf{k}, \lambda} \frac{f_{m, \mathbf{k}, \lambda} - f_{-m, \mathbf{k}, \lambda}}{E_{m, \mathbf{k}, \lambda} - E_{-m, \mathbf{k}, \lambda}}, \quad (47)$$

that follows from the self-consistency equation (17). Using the relation (47) we write the sums $\Pi_{ss}(\mathbf{q}, \omega) + 1/g$ ($s = 1, 2$) in the form

$$\begin{aligned} \Pi_{ss}(\mathbf{q}, \omega) + \frac{1}{g} &= \Pi_{ss}^{(R)}(\mathbf{q}, \omega) \\ &= \frac{1}{S} \sum_{\nu_1, \nu_2} \left[\delta_{\mathbf{k}_2, \mathbf{k}_1 + \mathbf{q}} \Phi_{\nu_1 \nu_2}^{ss} \frac{1 + \lambda_1 \lambda_2 \cos(\chi_{\mathbf{k}_1} - \chi_{\mathbf{k}_2})}{2} \frac{f_{\nu_1} - f_{\nu_2}}{E_{\nu_1} - E_{\nu_2} - \hbar(\omega + i\gamma)} - \delta_{\mathbf{k}_1, \mathbf{k}_2} \delta_{m_1, -m_2} \delta_{\lambda_1, \lambda_2} \frac{f_{\nu_1} - f_{\nu_2}}{E_{\nu_1} - E_{\nu_2}} \right]. \end{aligned} \quad (48)$$

The functions $\Pi_{11}^{(R)}(\mathbf{q}, \omega)$ and $\Pi_{22}^{(R)}(\mathbf{q}, \omega)$ calculated in the Dirac approximation do not diverge in the limit $k' \rightarrow \infty$ and this approximation can be applied.

Equating the determinant of the matrix in Eq. (46) to zero we obtain the dispersion equation for the eigenmode spectrum. The determinant is factorized into three multipliers. The first multiplier yields the equation

$$\varepsilon_+(\mathbf{q}, \omega) = 1 - V_+(q) \Pi_{00}(\mathbf{q}, \omega) = 0. \quad (49)$$

The quantity $\varepsilon_+(\mathbf{q}, \omega)$ can be interpreted as the dielectric function. It describes the screening of the scalar potential of a test charge $\rho_+^{\text{test}}(\mathbf{q}, \omega)$:

$$e^2 \varphi_+^{\text{src}}(\mathbf{q}, \omega) = \frac{V_+(q)}{\varepsilon_+(\mathbf{q}, \omega)} \rho_+^{\text{test}}(\mathbf{q}, \omega). \quad (50)$$

Eq. (50) follows from Eq. (44) written in the form $e^2 \varphi_+^{\text{src}}(\mathbf{q}, \omega) = V_+(q) [\rho_+^{\text{test}}(\mathbf{q}, \omega) + \rho_+^{\text{ind}}(\mathbf{q}, \omega)]$, where $\rho_+^{\text{ind}}(\mathbf{q}, \omega) = e^2 \Pi_{00}(\mathbf{q}, \omega) \varphi_+^{\text{src}}(\mathbf{q}, \omega)$ is the induced charge.

From the continuity equation for the charge we obtain the relation between the polarization function $\Pi_{00}(\mathbf{q}, \omega)$ and the longitudinal parallel current conductivity $\sigma_{+,xx}(\mathbf{q}, \omega)$:

$$\sigma_{+,xx}(q\mathbf{i}_x, \omega) = \frac{ie^2 \omega}{q^2} \Pi_{00}(q\mathbf{i}_x, \omega), \quad (51)$$

where \mathbf{i}_x is the unit vector along the x -axis.

Starting from the Maxwell equations and the matter equation for the current one arrives at the dispersion equation for the optical plasmon mode^{31,36}

$$1 + \frac{4\pi i \kappa_1}{\omega} \sigma_{+,xx}(q\mathbf{i}_x, \omega) + \frac{\varepsilon \kappa_1}{\kappa_2} \tanh \frac{\kappa_2 d}{2} = 0, \quad (52)$$

that differs from Eq. (49). In Eq. (52) $\kappa_1 = \sqrt{q^2 - \omega^2/c^2}$ and $\kappa_2 = \sqrt{q^2 - \varepsilon \omega^2/c^2}$. Eq. (52) accounts retarded effect. In the limit $\kappa_1 = \kappa_2 = q$ that corresponds to nonretarded (plasmon) approximation it is reduced to Eq. (49).

Thus, we have shown that order parameter fluctuations are decoupled from the fluctuations of φ_+ and do not influence the optical plasmon spectrum. The same result was obtained in Ref. 31 basing on the observation that the generalized Ward identity for the vertex function is satisfied with a bare vertex γ_+ , and the Feynmann diagram for the polarization function Π_{00} can be calculated with bare vertexes. The consideration³¹ was heuristic in its nature. Here we confirm its validity. Going ahead we would say that the heuristic approach³¹ describes φ_- oscillations less accurately.

It was shown³¹ that in the general case Eq. (49) has two solutions, one is below the gap ($\hbar\omega < 2\Delta_0$), and the other, above the gap ($\hbar\omega > 2\Delta_0$). To illustrate this property we consider the dielectric loss function. This function is defined as

$$L_+(\mathbf{q}, \omega) = -\text{Im} \left[\frac{1}{\varepsilon_+(\mathbf{q}, \omega)} \right]. \quad (53)$$

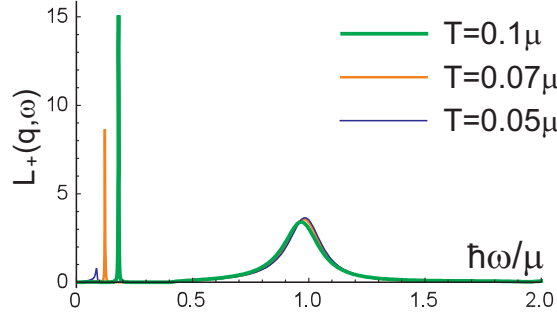


FIG. 1. Frequency dependence of the dielectric loss function (53) at $T = 0.1\mu$, 0.07μ , 0.05μ , $q = 0.1k_F$, $\Delta_0 = 0.2\mu$ and $\gamma = 10^{-3}\mu$

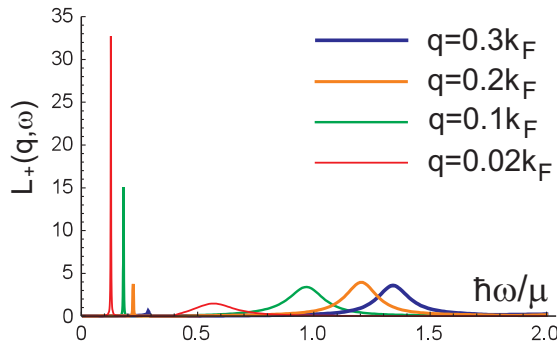


FIG. 2. Frequency dependence of the dielectric loss function (53) at $T = 0.1\mu$, $q = 0.02k_F$, $0.1k_F$, $0.2k_F$, $0.3k_F$, $\Delta_0 = 0.2\mu$ and $\gamma = 10^{-3}\mu$

The function (53) determines relative losses of energy of oscillations of a test charge ρ_+^{test} . The peaks in the ω -dependence of $L_+(q, \omega)$ at fixed q correspond to the eigenmodes. A half-width of the peak at its half-height gives the damping rate for the corresponding mode.

The frequency dependence of the dielectric loss function (53) for the same q and three different temperatures is shown in Fig. 1. The same dependence at fixed temperature and four different q is shown in Fig. 2. Figs. 1 and 2 illustrate that the lower mode is a weakly damped mode and its spectrum and the damping rate are very sensitive to the temperature. The lower mode disappears at low temperatures and at large wave vectors. One can also see that the upper mode has much larger damping rate. At constant Δ_0 the frequency and the damping rate of the upper mode is unsensitive to variations of the temperature. At $\Delta_0 \rightarrow 0$ the frequency of the upper mode approaches the frequency of the optical plasmon mode in the normal state.

The second multiplier in the determinant of the matrix in Eq. (46) yields the dispersion equation

$$\Pi_{11}^{(R)}(\mathbf{q}, \omega)\Pi_{22}^{(R)}(\mathbf{q}, \omega) + [\Pi_{12}(\mathbf{q}, \omega)]^2 = 0. \quad (54)$$

Equation (54) describes the oscillations of difference of two order parameters: $\Delta_\uparrow - \Delta_\downarrow$. Such oscillations are uncoupled from the scalar potential oscillations.

In the theory of superconductivity the eigenmodes that correspond to oscillations of the phase and the modulus of the order parameter are known as the Anderson-Bogoliubov mode^{37,38} and the Schmid³⁹ mode. Since in common superconductors the oscillations of the phase of the order parameter are coupled to plasma (scalar potential) oscillations, a genuine Anderson-Bogoliubov mode can emerge only in neutral Fermi superfluids. In counterflow superconductors the presence of two superconducting components allows to realize the Anderson-Bogoliubov mode. To visualize the

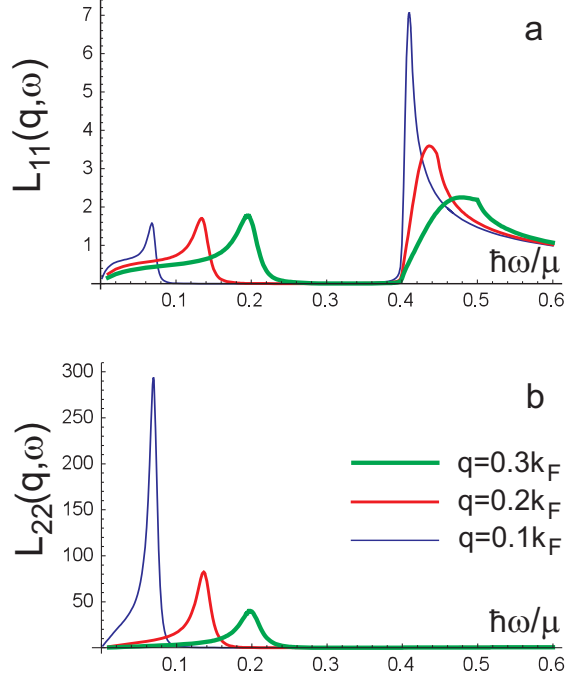


FIG. 3. Frequency dependence of the energy loss functions (55), (56) in μ/gk_F^2 units at $T = 0.1\mu$, $q = 0.1k_F$, $0.2k_F$, $0.3k_F$, $\Delta_0 = 0.2\mu$ and $\gamma = 10^{-3}\mu$

Anderson-Bogoliubov and the Schmid modes we introduce the functions

$$L_{11}(\mathbf{q}, \omega) = \frac{1}{g} \text{Im} \left[\frac{1}{\Pi_{11}^{(R)}(\mathbf{q}, \omega) + \frac{[\Pi_{12}(\mathbf{q}, \omega)]^2}{\Pi_{22}^{(R)}(\mathbf{q}, \omega)}} \right], \quad (55)$$

$$L_{22}(\mathbf{q}, \omega) = \frac{1}{g} \text{Im} \left[\frac{1}{\Pi_{22}^{(R)}(\mathbf{q}, \omega) + \frac{[\Pi_{12}(\mathbf{q}, \omega)]^2}{\Pi_{11}^{(R)}(\mathbf{q}, \omega)}} \right]. \quad (56)$$

These functions can be interpreted as analogs of the energy loss function (53). They describe losses of energy under externally driven oscillations of the amplitude and the phase of the order parameter. The frequency dependence of the function $L_{11}(\mathbf{q}, \omega)$ at three different q and $T = 0.1\mu$ is shown in Fig. 3a. The same dependence for the function $L_{22}(\mathbf{q}, \omega)$ is given in Fig. 3b.

The function $L_{22}(\mathbf{q}, \omega)$ has one peak at $\omega_{AB}(q) \approx qv_F/\sqrt{2}$. It is just the dispersion relation for the Anderson-Bogoliubov mode in two dimensions. The function $L_{11}(\mathbf{q}, \omega)$ has two peaks, one is at $\hbar\omega \approx 2\Delta_0$ that corresponds to the Schmid mode, and the other at $\omega \approx qv_F/\sqrt{2}$ that corresponds to the Anderson-Bogoliubov mode. The Anderson-Bogoliubov peak in $L_{11}(\mathbf{q}, \omega)$ emerges due to the hybridization of amplitude and phase oscillations in the model considered (in conventional superconductors these two modes are decoupled from each other³⁵). At large q the peak that corresponds to the Schmid mode washes out.

In Fig. 4 we present frequency dependencies of the energy loss functions $L_{11}(\mathbf{q}, \omega)$ and $L_{22}(\mathbf{q}, \omega)$ at $T = 0$. One can see that the positions of the Anderson-Bogoliubov peak remain practically unchanged under variation in temperature. At the same time lowering in temperature results in an essential narrowing of this peak that signals for a decrease of the damping rate of the Anderson-Bogoliubov mode.

The third multiplier in the determinant of the matrix in Eq. (46) yields the dispersion equation

$$\left[\Pi_{11}^{(R)}(\mathbf{q}, \omega) \Pi_{22}^{(R)}(\mathbf{q}, \omega) + [\Pi_{12}(\mathbf{q}, \omega)]^2 \right] [1 - V_-(q) \Pi_{33}(\mathbf{q}, \omega)]$$

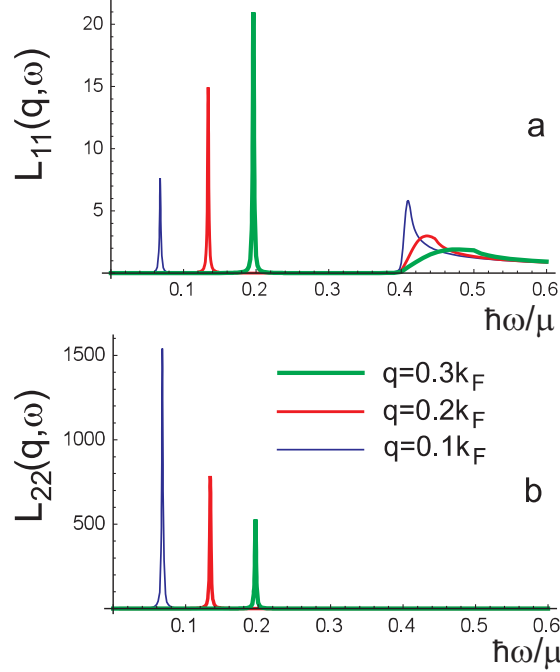


FIG. 4. The same as in Fig. 3 at $T = 0$.

$$-V_-(q) \left[\Pi_{11}^{(R)}(\mathbf{q}, \omega) [\Pi_{23}(\mathbf{q}, \omega)]^2 - \Pi_{22}^{(R)}(\mathbf{q}, \omega) [\Pi_{13}(\mathbf{q}, \omega)]^2 + 2\Pi_{12}(\mathbf{q}, \omega) \Pi_{13}(\mathbf{q}, \omega) \Pi_{23}(\mathbf{q}, \omega) \right] = 0. \quad (57)$$

One can see that at $V_-(q) = 0$ (that corresponds to $d = 0$) Eq. (57) coincides with Eq. (54).

At $V_-(q) \neq 0$ Eq. (57) can be rewritten in the form

$$\varepsilon_-(\mathbf{q}, \omega) = 1 - V_-(q) \Pi_-(\mathbf{q}, \omega) = 0, \quad (58)$$

where

$$\Pi_-(\mathbf{q}, \omega) = \Pi_{33}(\mathbf{q}, \omega) + \frac{\Pi_{11}^{(R)}(\mathbf{q}, \omega) [\Pi_{23}(\mathbf{q}, \omega)]^2 - \Pi_{22}^{(R)}(\mathbf{q}, \omega) [\Pi_{13}(\mathbf{q}, \omega)]^2 + 2\Pi_{12}(\mathbf{q}, \omega) \Pi_{13}(\mathbf{q}, \omega) \Pi_{23}(\mathbf{q}, \omega)}{\Pi_{11}^{(R)}(\mathbf{q}, \omega) \Pi_{22}^{(R)}(\mathbf{q}, \omega) + [\Pi_{12}(\mathbf{q}, \omega)]^2}. \quad (59)$$

The function $\Pi_-(\mathbf{q}, \omega)$ can be interpreted as a polarization function "dressed" by the order parameter fluctuations. The dielectric function $\varepsilon_-(\mathbf{q}, \omega)$ determines screening of the electrostatic field of a test charge $\rho_-^{\text{test}} = \rho_1^{\text{test}} - \rho_2^{\text{test}}$: $e^2 \varphi_-^{\text{src}}(\mathbf{q}, \omega) = V_-(q) \rho_-^{\text{test}}(\mathbf{q}, \omega) / \varepsilon_-(\mathbf{q}, \omega)$.

Having the expression for the polarization function $\Pi_-(\mathbf{q}, \omega)$ one gets the counterflow conductivity

$$\sigma_{-,xx}(q\mathbf{i}_x, \omega) = \frac{ie^2 \omega}{q^2} \Pi_-(q\mathbf{i}_x, \omega). \quad (60)$$

The dispersion equation for the acoustic TM mode obtained from the Maxwell equations has the form^{31,36}

$$\left(1 + \frac{4\pi i \kappa_1 \sigma_{-,xx}(q\mathbf{i}_x, \omega)}{\omega} \right) \tanh \frac{\kappa_2 d}{2} + \frac{\varepsilon \kappa_1}{\kappa_2} = 0. \quad (61)$$

In the nonretarded approximation ($\kappa_1 = \kappa_2 = q$) Eq. (61) reduces to Eq. (58).

Eq. (58) yields the spectrum of the order parameter oscillations coupled to the scalar potential oscillations. In conventional superconductors the mode that corresponds to such oscillations is known as the Carlson-Goldman mode⁴⁰.

We analyze Eq. (58) considering the energy loss function

$$L_-(\mathbf{q}, \omega) = -\text{Im} \left[\frac{1}{\varepsilon_-(\mathbf{q}, \omega)} \right]. \quad (62)$$

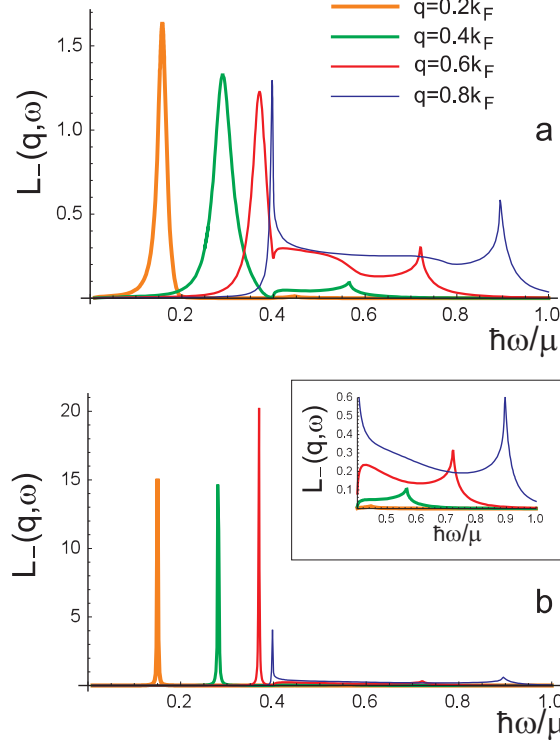


FIG. 5. Frequency dependence of the energy loss function (62) at $T = 0.1\mu$ (a) and $T = 0$ (b). The high-frequency peaks at $T = 0$ are shown in the inset in another scale.

The frequency dependence of $L_-(\mathbf{q}, \omega)$ for four different wave vectors ($q = 0.2k_F, 0.4k_F, 0.6k_F, 0.8k_F$) at $T = 0.1\mu$ and $\Delta_0 = 0.2\mu$ is shown in Fig. 5a. The other parameters are $\gamma = 10^{-3}\mu$, $dk_F = 0.1$ and $\varepsilon = 4$. One can see that this dependence contains two peaks, one is below the gap $2\Delta_0$ and the other, above the gap. The low-frequency peak is considerably narrower than the high-frequency one. In similarity with the φ_+ oscillation spectrum, the φ_- oscillation spectrum contains two modes. The lower mode has the acoustic dispersion relation at small wave vectors and its dispersion curve saturates at the energy $2\Delta_0$ at large wave vectors. This mode can be interpreted as an analog of the Carlson-Goldman mode.

At given q the frequency of the lower (Carlson-Goldman) mode is larger than the frequency of the Anderson-Bogoliubov mode. The velocity of this mode can be smaller than v_F , in difference with the acoustic plasmon velocity in the normal state that is always higher than v_F ⁴¹. It can be understood as follows. In the normal state the mode with $\omega < v_F q$ experiences a strong Landau damping. In the paired state the Landau damping is suppressed at $\hbar\omega < 2\Delta_0$ ³¹. Thus, a propagating mode with the velocity $s < v_F$ cannot emerge in the normal state, but there is no such a restriction in the paired state.

The high-frequency peak in Fig. 5a is well resolved only at sufficiently large wave vectors. This peak can be interpreted as a residual normal state acoustic plasmon peak that at $\Delta_0 \rightarrow 0$ is transformed into the normal state acoustic plasmon peak.

The frequency dependence of $L_-(\mathbf{q}, \omega)$ at $T = 0$ is shown in Fig. 5b. One can see that lowering in temperature results in a considerable decrease of the damping rate of the Carlson-Goldman mode. At the same time the frequency of this mode remains practically unchanged under variation in temperature (at $\Delta_0 = \text{const}$).

VI. CONCLUDING REMARKS

We have shown that in the model with contact interaction the linear response equations that account fluctuations of the order parameter of the electron-hole pairing can be presented in form of algebraic equations. We find that explicit accounting of the order parameter fluctuations allows to describe properly the spectrum of φ_- oscillations. We show

that this spectrum contains two branches. The upper branch can be interpreted as a residual normal state acoustic plasmon, while the lower branch, as an analog of the Carlson-Goldman mode. We show that the Anderson-Bogoliubov and Schmid modes are also present in the spectrum of the counterflow superconductor. These modes are associated with out-of-phase oscillations of the order parameters of two superconducting components.

Our approach can be easily generalized to describe eigenmodes in the double bilayer graphene system. The polarization functions for the double bilayer graphene are obtained from Eq. (38) under substitution $\xi_{\mathbf{k},\lambda} \approx \lambda \hbar^2 k'^2 / 2m - \mu$ and $\chi_{\mathbf{k}} \approx \mp 2\theta_{\mathbf{k}'}$, where m is the effective mass in the bilayer graphene. Preliminary study shows that the double bilayer graphene system with the electron-hole pairing demonstrates the same collective mode systematics.

We emphasize that our approach cannot be applied to the system with low density of carriers and a large gap between the valence and conducting bands. The latter system is described^{24,42,43} as a two-component superfluid gas of weakly interacting excitons. Its spectrum contains soft collective modes that signals for an instability with respect to spatial separations of components or with respect to a transition to a Wigner crystal state^{24,43}. The system considered in this paper is free from such instabilities.

ACKNOWLEDGEMENT

This study was supported by the grant of the Ukraine State Fund for Fundamental Research (project No. 33683).

* fil@isc.kharkov.ua

- ¹ S. I. Shevchenko, *Fiz. Nizk. Temp.* **2**, 505 (1976) [*Sov. J. Low Temp. Phys.* **2**, 251 (1976)].
- ² Yu. E. Lozovik and V. I. Yudson, *Zh. Eksp. Teor. Fiz.* **71**, 738 (1976) [*Sov. Phys. JETP* **44**, 389 (1976)].
- ³ D. V. Fil and S. I. Shevchenko, *Fiz. Nizk. Temp.* **44**, 1111 (2018) [*Low Temp. Phys.* **44**, 867 (2018)].
- ⁴ M. Kellogg, J. P. Eisenstein, L. N. Pfeiffer, and K. W. West, *Phys. Rev. Lett.* **93**, 036801 (2004).
- ⁵ E. Tutuc, M. Shayegan, and D. A. Huse, *Phys. Rev. Lett.* **93**, 036802 (2004).
- ⁶ R. D. Wiersma, J. G. S. Lok, S. Kraus, W. Dietsche, K. von Klitzing, D. Schuh, M. Bidder, H. - P. Tranitz, and W. Wegscheider, *Phys. Rev. Lett.* **93**, 266805 (2004).
- ⁷ J. P. Eisenstein, *Ann. Rev. Condensed Matter Phys.* **5**, 159 (2014).
- ⁸ I. B. Spielman, J. P. Eisenstein, L. N. Pfeiffer, and K. W. West, *Phys. Rev. Lett.* **87**, 036803 (2001).
- ⁹ D. Nandi, A. D. K. Finck, J. P. Eisenstein, L. N. Pfeiffer, and K. W. West, *Nature* **488**, 481 (2012).
- ¹⁰ A. F. Croxall, K. Das Gupta, C. A. Nicoll, M. Thangaraj, H. E. Beere, I. Farrer, D. A. Ritchie, and M. Pepper, *Phys. Rev. Lett.* **101**, 246801 (2008).
- ¹¹ J.A. Seamons, C. P. Morath, J. L. Reno, and M. P. Lilly, *Phys. Rev. Lett.* **102**, 026804 (2009).
- ¹² A. Gamucci, D. Spirito, M. Carrega, B. Karmakar, A. Lombardo, M. Bruna, L. N. Pfeiffer, K. W. West, A. C. Ferrari, M. Polini, and V. Pellegrini, *Nat. Commun.* **5**, 5824 (2014).
- ¹³ G. W. Burg, N. Prasad, K. Kim, T. Taniguchi, K. Watanabe, A. H. MacDonald, L. F. Register, and E. Tutuc, *Phys. Rev. Lett.* **120**, 177702 (2018).
- ¹⁴ Yu. E. Lozovik and A. A. Sokolik, *Pis'ma v ZhETF* **87** 61 (2008) [*JETP Lett.* **87**, 55 (2008)].
- ¹⁵ H. Min, R. Bistritzer, J.-J. Su, and A. H. MacDonald, *Phys. Rev. B* **78**, 121401 (R) (2008)
- ¹⁶ B. Seradjeh, H. Weber, and M. Franz, *Phys. Rev. Lett.* **101**, 246404 (2008).
- ¹⁷ M. P. Mink, H. T. C. Stoof, R. A. Duine, and A. H. MacDonald, *Phys. Rev. B* **84**, 155409 (2011).
- ¹⁸ I. Sodemann, D. A. Pesin, and A. H. MacDonald, *Phys. Rev. B* **85**, 195136 (2012).
- ¹⁹ Yu. E. Lozovik, S. L. Ogarkov, and A. A. Sokolik, *Phys. Rev. B* **86**, 045429 (2012).
- ²⁰ A. Perali, D. Neilson, and A. R. Hamilton, *Phys. Rev. Lett.* **110**, 146803 (2013).
- ²¹ J.-J. Su, A. H. MacDonald, *Phys. Rev. B* **95** 045416 (2017).
- ²² S. Conti, A. Perali, F. M. Peeters, and D. Neilson, *Phys. Rev. Lett.* **119**, 257002 (2017).
- ²³ M. Zarenia, A. Perali, D. Neilson, and F.M. Peeters, *Sci. Rep.* **4** 7319 (2014).
- ²⁴ F. C. Wu, F. Xue, and A. H. MacDonald, *Phys. Rev. B* **92**, 165121 (2015).
- ²⁵ B. Debnath, Y. Barlas, D. Wickramaratne, M. R. Neupane, and R. K. Lake, *Phys. Rev. B* **96**, 174504 (2017).
- ²⁶ O. L. Berman and R. Ya. Kezerashvili, *Phys. Rev. B* **96**, 094502 (2017).
- ²⁷ O. L. Berman, G. Gumbs, and R. Ya. Kezerashvili, *Phys. Rev. B* **96**, 014505 (2017).
- ²⁸ B. Seradjeh, J. E. Moore, and M. Franz, *Phys. Rev. Lett.* **103**, 066402 (2009).
- ²⁹ D. K. Efimkin, Yu. E. Lozovik, and A. A. Sokolik, *Phys. Rev. B* **86**, 115436 (2012).
- ³⁰ K. V. Germash and D. V. Fil, *Phys. Rev. B* **91**, 115442 (2015).
- ³¹ K. V. Germash and D. V. Fil, *Phys. Rev. B* **93**, 205436 (2016).
- ³² K. V. Germash and D. V. Fil, *EPL* **118**, 67008 (2017).
- ³³ Y. Nambu, *Phys. Rev.* **117**, 648 (1960).
- ³⁴ J. R. Schrieffer, *Theory of Superconductivity* (Benjamin, New York, 1964).
- ³⁵ I. O. Kulik, O. Entin-Wohlman, R. Orbach, *J. Low Temp. Phys.* **43**, 591 (1981).

³⁶ Yu.V. Bludov, A. Ferreira, N. M. R. Peres, M. I. Vasilevskiy, Int. J. Mod. Phys. B **27**, 1341001 (2013).

³⁷ P. W. Anderson, Phys. Rev. **112**, 1900 (1958).

³⁸ N. N. Bogoljubov, V. V. Tolmachov, D. V. Shirkov, Fortschritte der Physik **6**, 605 (1958).

³⁹ A. Schmid, Phys. kondens. Materie **8**, 129 (1968).

⁴⁰ R. V. Carlson and A. M. Goldman, Phys. Rev. Lett. **34**, 11 (1975).

⁴¹ R. E. V. Profumo, R. Asgari, M. Polini, A. H. MacDonald, Phys. Rev. B **85**, 085443 (2012).

⁴² Yu. L. Lozovik and O. L. Berman, Zh. Eksp. Teor. Fiz. **111**, 1879 (1997) [J. Exp. Theor. Phys. **84**, 1027 (1997)].

⁴³ D. V. Fil and S. I. Shevchenko, Fiz. Nizk. Temp. **42**, 1013 (2016) [Low Temp. Phys. **42**, 794 (2016)].